Advanced and Sustainable Technologies
ASET
E-ISSN 2976-2294
Volume 3, No 1, June 2024 [62-70]

Computational Fluid Dynamics Analysis on the Road Bike Using Different Flow Models under Extreme Inlet Velocity

Keat Ming Tan[1*]

[1]Faculty of Mechanical Engineering & Technology, Universiti Malaysia Perlis (UniMAP), 02600 Arau, Perlis, Malaysia

Received 2 April 2024, Revised 25 April 2024, Accepted 8 May 2024

ABSTRACT

At high velocities, the aerodynamic forces acting on the road bike and rider become more pronounced, potentially affecting stability and control. Riders might experience increased resistance, requiring more effort to maintain balance and direction. This research employs Computational Fluid Dynamics (CFD) to thoroughly examine the external aerodynamics of road bikes, focusing on pre-processing techniques and their impact on overall aerodynamic performance. The research applies CFD methods for geometry preparation, meshing, and material property definition within a structured workflow using a road bike model representative of the cycling industry via SimFlow software. Through systematic variations in extreme inlet velocities (40, 70, and 100 m/s) and the utilization of diverse turbulent models, k-ω Shear-Stress Transport (SST) and Reynolds-Averaged Navier-Stokes (RANS) with k-ε and k-ω, the study reveals intricate airflow patterns around the road bike. The results explain the complicated connection between turbulent models and inlet velocities and provide new information on critical aerodynamic parameters, such as pressure and maximum velocity of the road bike model.

Keywords: Road bike, Computational Fluid Dynamics, k-ω Shear-Stress Transport, Reynolds-Averaged Navier-Stokes.

1. INTRODUCTION

Computational Fluid Dynamics (CFD) plays a crucial role in advancing aerodynamics within the cycling industry, particularly in the design and optimization of road bikes. This study investigates the simulation of airflow around a road bike model, exploring the effects of varying inlet velocities and utilizing different turbulent models, including laminar [1], k-ω Shear-Stress Transport (SST) [2], Reynolds-Averaged Navier-Stokes (RANS) with k-ε [3], and RANS with k-ω [4]. Within the CFD software workflow, meticulous pre-processing steps are essential [5]. These steps include geometry preparation, meshing, defining material properties, and specifying initial and boundary conditions. The accuracy and reliability of the simulation outcomes are heavily dependent on the careful execution of these pre-processing stages [6].

Several studies [7, 8, 9, 10] have applied CFD methods to analyze the external aerodynamics of road bikes, focusing on different aspects of the CFD workflow, such as pre-processing, turbulence modeling, and post-processing. Pre-processing involves preparing the geometry, mesh, and material properties of the bike and the rider, which significantly affect the accuracy and reliability of the simulations. For instance, Crouch et al. [7] demonstrated the importance of meticulous pre-processing in achieving accurate simulations, detailing the intricate steps of geometry preparation, meshing, and material property definition within the CFD workflow. They also discussed the challenges and limitations of pre-processing, such as the complexity of the

*Corresponding author: tankming0000111@gmail.com

geometry, the trade-off between mesh quality and computational cost, and the uncertainty of the material properties.

Turbulence modeling is another crucial aspect of the CFD workflow, as it determines how the turbulent flow around the bike and rider is simulated. Different turbulence models have varying assumptions, strengths, and weaknesses and can yield different results for the same problem [11]. The RANS k-ε model is known for its robustness and computational efficiency, making it a popular choice for various engineering applications [12]. It assumes isotropic turbulence, simplifying the calculations, but may not capture all the nuances of turbulent flow, especially in regions with significant flow separation and reattachment. On the other hand, the RANS k-ω model, particularly in its Shear-Stress Transport (SST) variant, is designed to provide more accurate predictions in scenarios with strong adverse pressure gradients and flow separation [13]. It transitions smoothly between the k-ω model in the near-wall region and the k-ε model in the free stream, offering a balanced approach that enhances its predictive capabilities. Blocken et al. [14] compared the performance of different turbulence models, such as laminar, k-ω Shear-Stress Transport (SST), and Reynolds-Averaged Navier-Stokes (RANS) with k-ε and k-ω models, in simulating the aerodynamics of road bikes. They found that the k-ω SST model was the most suitable for this application, as it better-captured flow separation and reattachment, providing more accurate predictions of the drag coefficient and pressure distribution. They also emphasized the importance of validating CFD results with experimental data, such as wind tunnel tests or track measurements, to ensure the simulations' reliability and accuracy.

The current study focuses on the simulation analysis of a road bike using various extremely high inlet velocities, examining the effects of the RANS k-ε and k-ω turbulence models. The simulations were conducted using SimFlow software [15], a powerful computational fluid dynamics (CFD) analysis tool. By employing a range of high inlet velocities, this study aims to push the boundaries of typical aerodynamic simulations to explore the limits of the road bike's performance. The investigation involves a detailed comparison of the RANS k-ε and k-ω turbulence models, widely used in CFD for their ability to handle complex turbulent flows. By systematically adjusting inlet velocities and employing different turbulent models, this study aims to reveal changes in airflow patterns and their impact on critical parameters such as maximum velocity and pressure within the road bike model. The outcomes comprehensively analyze the dynamic interplay between inlet velocity and turbulence models. This analysis offers valuable insights for advancing aerodynamics and optimizing road bike design, contributing significantly to the broader field of aerodynamic research in road cycling.

2. MATERIAL AND METHODS

The simulation analysis was performed using SimFlow software. The road bike model's dimensions are 165 cm × 104 cm × 45 cm, as illustrated in Figure 1(a). To accurately capture the gradient around the bike, the model underwent refinement. The flow domain, with minimum extents of (-20, -5.2, 2.25) and maximum extents of (40, 20, 7), is created in SimFlow. The meshing was configured with divisions of (50, 15, 20), producing cell sizes of 1.2, 1.68, and 0.2375 cm along each axis, primarily using hexahedral elements. Approximately 97,000 cells were generated in total. The symmetrical meshed model is shown in Figure 1(b). Quality checks in SimFlow showed that the mesh had an acceptable aspect ratio, maximum skewness, and non-orthogonality.

The simulation assumed a steady-state and incompressible flow condition, using the SIMPLE solver and the RANS k-ω SST turbulence model. Boundary conditions included an inlet velocity (X+), a pressure outlet (X-), wall boundaries for the bike body and the bottom surface of the domain (Y-), and a symmetry plane on the Z- surface. The simulation achieved convergence after 200 iterations, with three extreme velocities (40, 70, and 100 m/s) analyzed in the first analysis. The simulation analysis was also extended to different turbulent models (RANS k-ε and k-ω).

(a) (b)

Figure 1: (a) Road bike geometry used in the CFD analysis and symmetrical meshed model.

3. RESULTS AND DISCUSSION

The simulation results of the road bike under extremely high inlet velocity are summarized in Table 1. When the inlet velocity is set to 100 m/s, the simulation reveals that the maximum velocity within the airflow around the road bike reaches 140 m/s. The maximum pressure climbs to 6400 Pa. Figure 2(a) illustrates the velocity distribution. Red areas denote the highest airflow impact, mainly concentrated around the road bike handlebar. This situation indicates that the handlebar area experiences the most significant aerodynamic forces, likely due to its position and shape, which disrupts and accelerates the incoming air. Conversely, blue areas in the figure suggest regions of lower airflow intensity, predominantly around the main body of the bike, where the streamlined design reduces air resistance and maintains smoother flow.

In contrast, Figure 2(b) depicts the pressure distribution. Green areas indicate normal pressure levels, representing the baseline aerodynamic load on the bike. Red areas, however, highlight regions of higher pressure intensity. These high-pressure zones are primarily located at the front of the bike and around crucial structural elements such as the handlebars and the front wheel. This distribution suggests that these parts of the bike face increased aerodynamic drag, necessitating careful design considerations to optimize performance and reduce resistance. The data from the simulations emphasize the critical areas of aerodynamic impact on the road bike. Both velocity and pressure changes particularly influence the handlebars and front structural components. A similar phenomenon was observed when the inlet velocity increased, as illustrated in Figures 3 and 4. The magnitude of the maximum velocity and pressure on the road bike body increased rapidly. Understanding these dynamics is essential for improving the bike's aerodynamic efficiency, ultimately enhancing speed and performance in real-world conditions.

Table 1: Maximum velocity and pressure acting on the road bike under various extremely high inlet velocities.

Extremely high inlet velocity (m/s)		**Flow model**	**Maximum Velocity (m/s)**	**Maximum Pressure (Pa)**
V_1	40	RANS *k*-ω-SST	56	1000
V_2	70		98	3100
V_3	100		140	6400

Several issues arise when the velocity becomes too high for the road bike. Aerodynamic drag increases significantly, making it harder for the rider to maintain speed and requiring more energy [16]. High-pressure zones at the front and around the handlebars create additional resistance and affect control. Turbulence and flow separation can occur, causing unsteady aerodynamic forces and reducing stability [17]. Excessive speeds may also impose stresses beyond the bike's structural limits, risking component failure. Moreover, high speeds can compromise the rider's ability to control the road bike effectively and increase physical fatigue. Therefore, optimizing the road bike's aerodynamic design is crucial to balance speed, stability, and safety.

The practical implications of the simulation results for road bikes under extremely high inlet velocities are significant for bike design and performance optimization. The findings highlight critical areas of aerodynamic impact, particularly around the handlebars and front structural components. The concentration of aerodynamic forces in these areas suggests the need for targeted design improvements to enhance aerodynamic efficiency and reduce resistance. For instance, modifying the shape or positioning of the handlebars could potentially minimize drag and improve overall bike performance. The observed increase in maximum velocity and pressure with higher inlet velocities underscores the importance of aerodynamic considerations in bike design. As inlet velocity increases, the aerodynamic forces exerted on the bike intensify, affecting both speed and stability. Designers and engineers must carefully balance these factors to optimize bike performance under varying conditions.

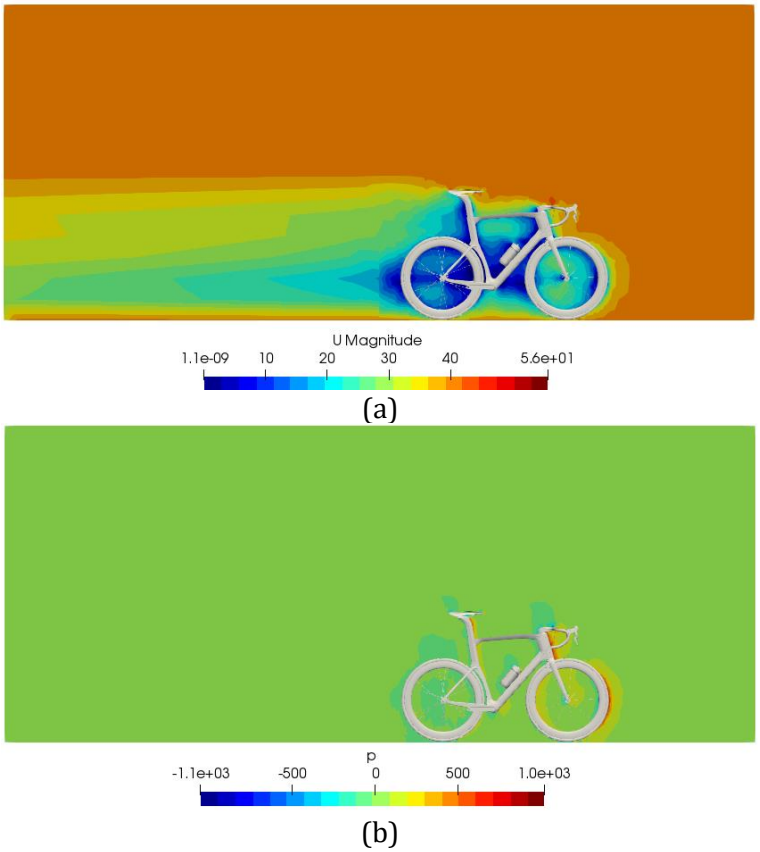

Figure 2: (a) Maximum velocity (m/s) and (b) maximum pressure (Pa) on the road bike at 40 m/s inlet velocity.

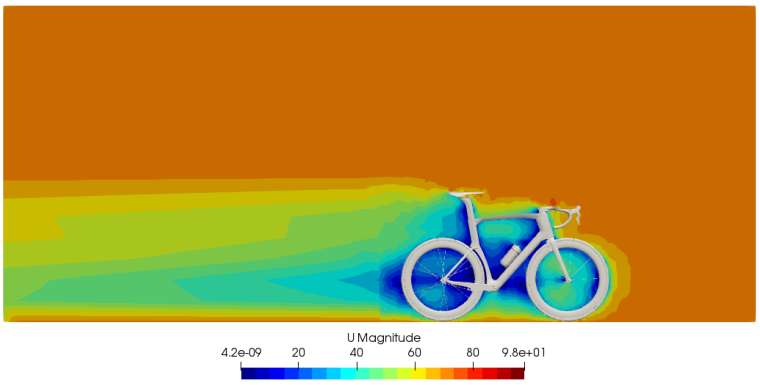

(a)

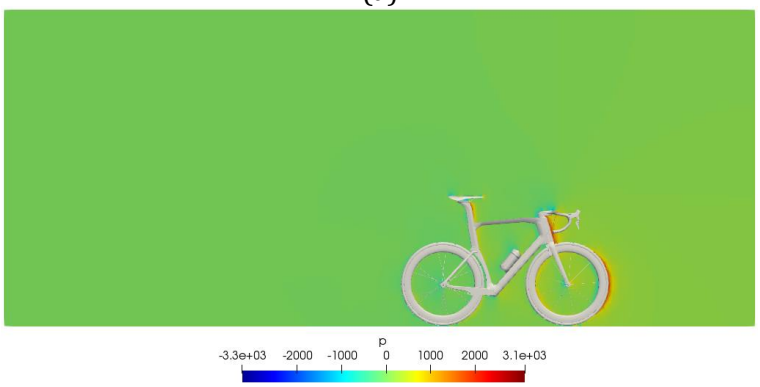

(b)

Figure 3: (a) Maximum velocity (m/s) and (b) maximum pressure (Pa) on the road bike at 70 m/s inlet velocity.

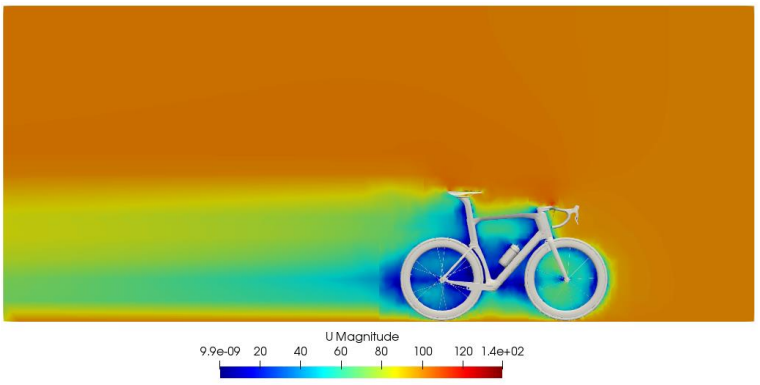

(a)

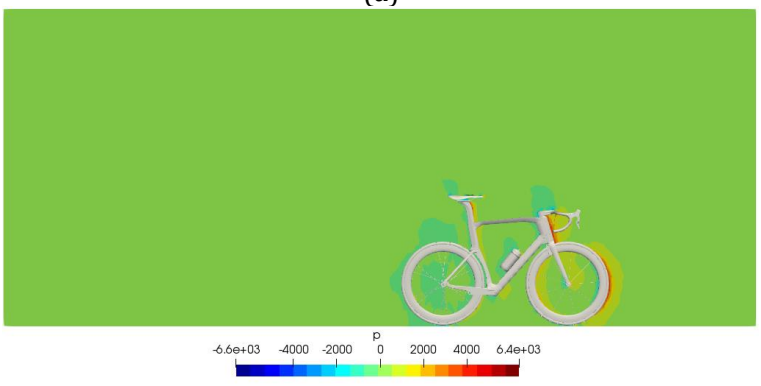

(b)

Figure 4: (a) Maximum velocity (m/s) and (b) maximum pressure (Pa) on the road bike at 100 m/s inlet velocity.

Besides, airflow and pressure distribution across different road bike parts provide valuable insights for aerodynamic optimization. Areas experiencing higher pressure intensity, such as the front of the bike and around critical structural elements, require particular attention to mitigate aerodynamic drag and improve overall efficiency. Implementing design modifications based on these insights could lead to significant performance enhancements in real-world cycling scenarios. Therefore, understanding airflow dynamics and pressure around road bikes under high velocities is essential for advancing aerodynamic efficiency and maximizing performance. By leveraging these findings, road bike manufacturers can develop innovative design solutions that enhance speed, agility, and rider comfort, ultimately providing cyclists a competitive edge in racing and recreational activities.

In the second analysis, two RANS turbulence models, k-ε and k-ω, were used to examine the effect on flow behavior at an inlet velocity of 20 m/s. The k-ε turbulence model resulted in a highest maximum velocity of 28 m/s and a maximum pressure of 250 Pa. Figure 5(a) shows the velocity distribution, where red areas indicate significant flow impact at the stem of the road bike, while blue areas show less flow impact throughout the bike. Conversely, the pressure distribution in Figure 5(b) reveals that green regions denote expected pressure impact, and red areas indicate more substantial pressure. Using the k-ω model, the maximum velocity reached 25 m/s, and the maximum pressure was 260 Pa. In Figure 6 (a), the maximum value in the color legend shows the highest velocity is 74 m/s. However, the velocity contour indicates that the realistic maximum velocity around the road bike is only 25 m/s. The color distributions for this model similarly highlight areas of intense flow and pressure. However, the values suggest that the k-ε model is more effective at capturing higher velocities. In contrast, the k-ω model provides slightly higher pressure readings. These differences underscore the importance of choosing an appropriate turbulence model for accurately simulating and understanding the complex aerodynamic behavior around the road bike at varying velocities.

Table 2: Maximum velocity and pressure acting on the road bike using different RANS turbulence models.

Flow model		**Constant inlet velocity (m/s)**	**Maximum Velocity (m/s)**	**Maximum Pressure (Pa)**
M_1	RANS (k-ε)	20	28	250
M_2	RANS (k-ω)		25	260

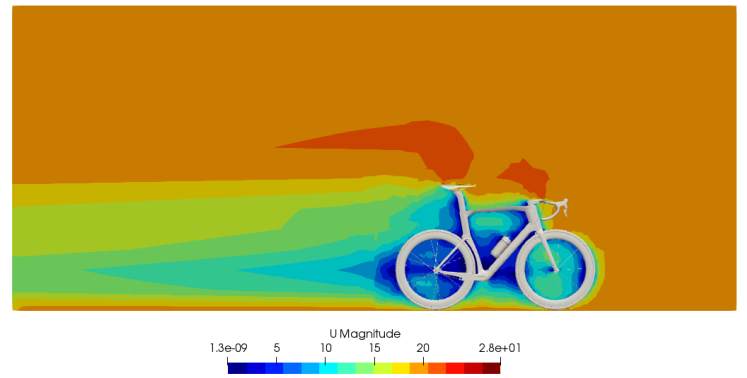

(a)

(b)

Figure 5: (a) Maximum velocity and (b) maximum pressure on the road bike at 20 m/s inlet velocity using RANS (k-ε) model.

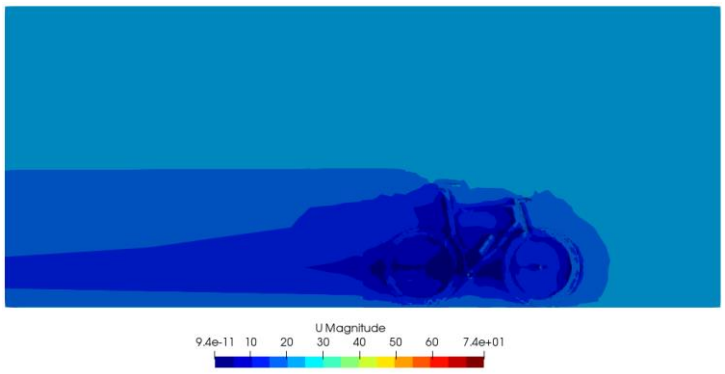

(a)

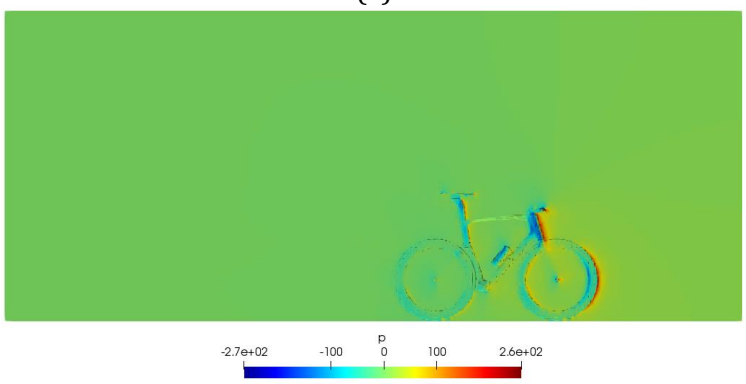

(b)

Figure 6: (a) Maximum velocity and (b) maximum pressure on the road bike at 20 m/s inlet velocity using RANS (k- ω) model.

4. CONCLUSION

In conclusion, this study successfully applied Computational Fluid Dynamics (CFD) to investigate the aerodynamic aspects impacted by the high inlet velocity. The objectives were achieved through a meticulous workflow, including geometry preparation, meshing, and material property definition. The road bike model, representative of the cycling industry, served as the focal point for this examination. Systematic adjustments of input velocities and applying various turbulent models clarified the detailed dynamics of the external airflow surrounding the road bike. The results revealed complex correlations between turbulent models, critical aerodynamic parameters, and inlet velocities, providing valuable insights into the interactions between maximum velocity and pressure in the road bike model. At extremely inlet velocities, the maximum velocity on the road bike body ranges from 56-140 m/s. The maximum pressure on the road bike is 1000-6400 Pa. This study demonstrated the efficacy of CFD in analyzing external aerodynamics and contributed essential knowledge for advancing the design and optimization of road bikes. Consequently, it enriches the broader field of aerodynamic research in road cycling.

ACKNOWLEDGEMENTS

The author sincerely appreciates the Faculty of Mechanical Engineering & Technology's invaluable support and resources throughout this research.

REFERENCES

[1] Jux, C., Sciacchitano, A., & Scarano, F. Tire dependence for the aerodynamics of yawed bicycle wheels. Journal of Wind Engineering and Industrial Aerodynamics, vol 233, (2023) p.105294.

[2] Yakkundi, V. K., & Mantha, S. S. Computational Analysis of" Drag & Lift" of a car With K-ε std, and K-ω SST (Shear Stress Transport) Turbulence Models & Effect of Mesh Refinement. CURIE Journal, vol 3, (2010).

[3] Fintelman, D. M., Hemida, H., Sterling, M., & Li, F. X. CFD simulations of the flow around a cyclist subjected to crosswinds. Journal of Wind Engineering and Industrial Aerodynamics, vol 144, (2015) pp. 31-41.

[4] Blocken, B., & Malizia, F. How much can roof-mounted bicycles on a following team car reduce cyclist drag?. Journal of Wind Engineering and Industrial Aerodynamics, vol 249, (2024) p.105723.

[5] Berger, M., & Cristie, V. CFD post-processing in Unity3D. Procedia Computer Science, vol 51, (2015) pp. 2913-2922.

[6] Li, L., Lange, C. F., Xu, Z., Jiang, P., & Ma, Y. Feature-based intelligent system for steam simulation using computational fluid dynamics. Advanced Engineering Informatics, vol 38, (2018) pp. 357-369.

[7] Crouch, T. N., Burton, D., LaBry, Z. A., & Blair, K. B. Riding against the wind: a review of competition cycling aerodynamics. Sports Engineering, vol 20, (2017) pp. 81-110.

[8] Godo, M., Corson, D., & Legensky, S. An aerodynamic study of bicycle wheel performance using CFD. In 47th AIAA aerospace sciences meeting including the new horizons forum and aerospace exposition, (2009) p. 322.

[9] Malizia, F., & Blocken, B. CFD simulations of an isolated cycling spoked wheel: impact of the ground and wheel/ground contact modeling. European Journal of Mechanics-B/Fluids, vol 82, (2020) pp. 21-38.

[10] van Druenen, T., & Blocken, B. CFD simulations of cyclist aerodynamics: Impact of computational parameters. Journal of Wind Engineering and Industrial Aerodynamics, vol 249, (2024) p.105714.

[11] Spalart, P. R. Strategies for turbulence modelling and simulations. International journal of heat and fluid flow, vol 21, issue 3 (2000) pp. 252-263.
[12] Xiao, H., & Cinnella, P. Quantification of model uncertainty in RANS simulations: A review. Progress in Aerospace Sciences, vol 108, (2019) pp. 1-31.
[13] Menter, F. R. Review of the shear-stress transport turbulence model experience from an industrial perspective. International journal of computational fluid dynamics, vol 23, issue 4 (2009) pp. 305-316.
[14] Blocken, B., van Druenen, T., Toparlar, Y., & Andrianne, T. CFD analysis of an exceptional cyclist sprint position. Sports Engineering, vol 22, (2019) pp. 1-11.
[15] Rey-Martinez, J., Altuna, X., Cheng, K., Burgess, A. M., & Curthoys, I. S. Computing endolymph hydrodynamics during head impulse test on normal and hydropic vestibular labyrinth models. Frontiers in Neurology, vol 11, (2020) p.516889.
[16] Kyle, C. R. Energy and aerodynamics in bicycling. Clinics in sports medicine, vol 13, issue 1 (1994) pp. 39-73.
[17] Malizia, F., & Blocken, B. Cyclist aerodynamics through time: Better, faster, stronger. Journal of Wind Engineering and Industrial Aerodynamics, vol 214, (2021) p.104673.

Conflict of interest statement: The author declares no conflict of interest.

Author contributions statement: Conceptualization; Methodology; Software; Analysis; Investigation; Writing & Editing, K.M. Tang